Interaction between Biotin Lipids and Streptavidin in Monolayers: Formation of Oriented Two-Dimensional Protein Domains Induced by Surface Recognition†

R. Blankenburg, P. Meller, H. Ringsdorf,* and C. Salesse
Institut für Organische Chemie, Universität Mainz, D-6500 Mainz, FRG
Received January 13, 1989; Revised Manuscript Received May 9, 1989

ABSTRACT: Highly specific ligand-receptor interactions generally characterize surface recognition reactions. Such processes can be simulated by streptavidin–biotin-specific binding. Biotin lipids have thus been synthesized, and their interaction with streptavidin (or avidin) at the air–water interface was directly shown by measurement of surface pressure isotherms and fluorescence microscopy. These proteins interact with the biotin lipid monolayer via specific binding or nonspecific adsorption. Both phenomena were clearly distinguished by use of the inactivated form of streptavidin. The binding of fluorescein-labeled streptavidin to monolayers was also directly observed by fluorescence microscopy. The fluorescence of the protein domains is directly related to the state of polarization of the exciting light. This anisotropy can only be explained by the formation of oriented two-dimensional biotin lipid–streptavidin domains.

Surface recognition processes involve highly specific binding of ligand molecules with membrane-incorporated receptors. Specific binding of monoclonal antibody, cholera toxin, and ribonucleotide reductase to lipid hapten (Uzgiris & Kornberg, 1983; Uzgiris, 1987), ganglioside GM1 (Reed et al., 1987; Ribi et al., 1988), and nucleolipid (Ribi et al., 1987), respectively, has been shown to induce these proteins to self-organize into two-dimensional crystals. In the present study, the well-known high-affinity, specific binding of biotin to the protein streptavidin was used to simulate such surface recognition processes.

Streptavidin is a protein which is comprised of four identical subunits, each binding one biotin molecule. The affinity binding between streptavidin and biotin is so high ($K_a \sim 10^{15}$ mol^{-1}) that the formation of this complex can be regarded as nearly irreversible (Green, 1975; Garlick & Giese, 1988), on a scale nearly comparable to a covalent bond. The streptavidin–biotin system is therefore ideal for simulating surface recognition processes like the antigen–antibody reaction where affinity binding is also very high. The high-affinity binding of this system has found many applications [for a review, see Wilchek and Bayer (1988)], e.g., in affinity chromatography (Cuatrecasas & Wilchek, 1968) and in attaching antibodies to liposomes (Loughrey et al., 1987), precipitating liposomes (Hashimoto et al., 1986), or targeting cells with liposomes (Bayer et al., 1979).

In the present surface recognition system, biotin acts as the membrane-incorporated receptor and streptavidin as the ligand. A series of new (compounds **4–8**) as well as already-known (compounds **1–3**; Bayer et al., 1979) biotin lipids have, therefore, been synthesized, where biotin is linked to the headgroup of the molecule (Chart I).

The specific binding of subphase-solubilized streptavidin with monolayers of different biotin lipids has then been discriminated from nonspecific adsorption by means of surface pressure isotherms. Moreover, through specific recognition, fluorescently labeled streptavidin spontaneously organizes in the plane of the monolayer to form large protein domains, directly visible in situ by fluorescence microscopy at the gas–water interface.

Materials and Methods

Materials. *N*-Hydroxysuccinimide, dicyclohexylcarbodiimide, dioctadecylamine, octadecanol, L-cysteine, and cysteamine were purchased from Fluka. Biotin, DMPE,[1] DPPE, DSPE, FITC, (fluorescein isothiocyanate), octyl glucoside, and emulphogen BC-720 were purchased from Sigma. Avidin and streptavidin were purchased from Belovo/Belgium and Boehringer Mannheim, respectively. For flash chromatography, silica gel with a 0.04–0.06-mm particle diameter (Merck) was used.

Synthesis of the Biotinylated Phospholipids. The three biotin lipids **1–3** were prepared according to the method described by Bayer et al. (1979). After the reaction, the crude lipid mixture was purified by flash chromatography with the following solvent mixture: $CHCl_3/MeOH/H_2O$ (65/25/4).

N-Biotinyldimyristoylphosphatidylethanolamine (**1**): yield 89%; mp 163 °C dec; ^1H 400-MHz NMR ($CDCl_3$) δ 0.85 (t, 6 H, $-CH_3$), 1.25 (m, 40 H, CH_2), 1.43 (m, 2 H, $NHCOCH_2CH_2$), 1.59 (s, 4 H, CH_2CH_2OOC), 1.70 [m, 4 H, $COCH_2CH_2(CH_2)_2CH$], 2.28 (m, 6 H, CH_2OOC and $NHCOCH_2$), 2.61 (s, 2 H, CH_2NHCO), 2.72 and 2.87 (d and dd, 2 H, SCH_2CH), 3.13 (m, 1 H, SCH), 3.91 [m, 4 H, $PO_4(CH_2)_2$], 4.12 and 4.38 (dd and d, 2 H, $COOCH_2CH$), 4.31 and 4.48 [m, 2 H, $(CH)_2(NH)_2CO$], 5.20 (m, 1 H, COOCH), 6.63 and 6.97 [s, 2 H, $(NH)_2CO$], 7.71 (m, 1 H, CONH); IR (KBr) 2919 and 2851 (C–H), 1740 (C=O ester), 1718 (C=O urea), 1700 and 1559 (C=O amide), 1468 (C–H) cm^{-1}. Anal. Calcd for $C_{43}H_{80}O_{10}N_3SP$: C, 60.18; H, 8.92; N, 4.89; S, 3.74; P, 3.62. Found: C, 59.76; H, 9.00; N, 4.48; S, 3.20; P, 3.50. The spectra of biotin lipids **2** and **3** are similar to those of biotin lipid **1**.

Synthesis of the Precursors of the Biotinylated Amino Lipids. Dioctadecylamine (DODA) was purified by recrystallization twice from ethyl acetate. Biotinyl-*N*-hydroxy-

† This research was supported by a grant from the Bundesministerium für Forschung und Technologie. C.S. was the recipient of a postdoctoral fellowship from the Natural Sciences and Engineering Research Council of Canada.

[1] Abbreviations: DMPE, dimyristoylphosphatidylethanolamine; DPPE, dipalmitoylphosphatidylethanolamine; DSPE, distearoylphosphatidylethanolamine; FITC, fluorescein isothiocyanate; DODA, dioctadecylamine; BNHS, biotinyl-*N*-hydroxysuccinimide; DMF, dimethylformamide; TLC, thin-layer chromatography.

0006-2960/89/0428-8214$01.50/0

Chart I: Synthesized Biotin Lipids **1**–**8** and Water-Soluble Biotin Derivatives **9** and **10**

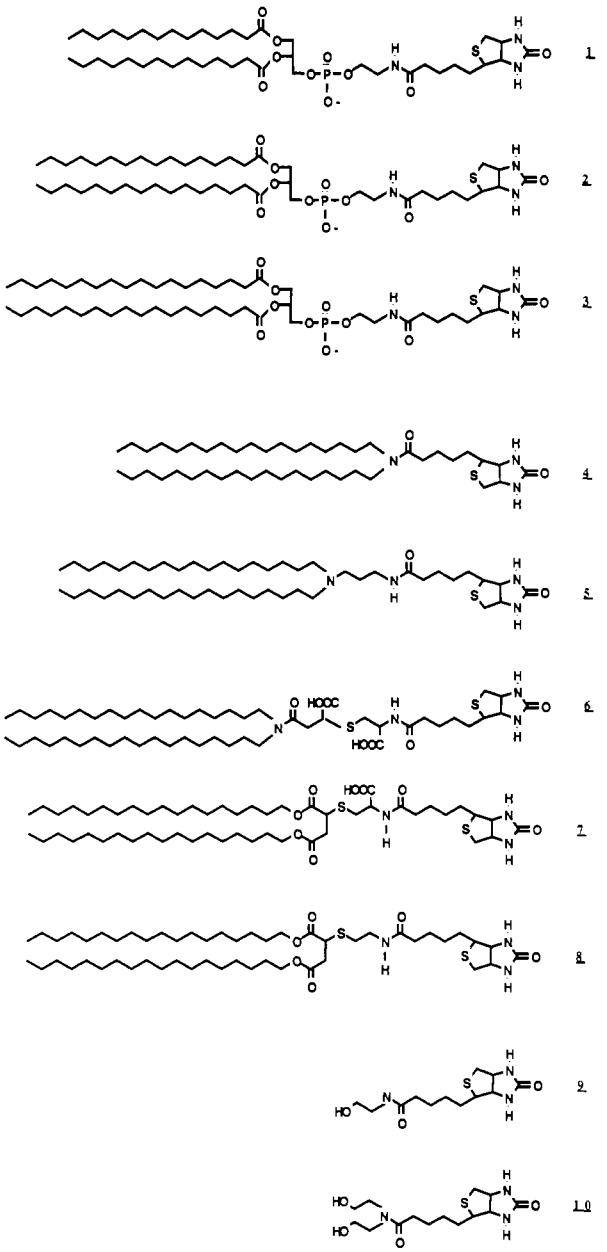

succinimide (BNHS) was prepared from biotin and *N*-hydroxysuccinimide according to Bayer and Wilchek (1974).

The two amino acid lipids (precursors of lipids **6** and **7**) were synthesized according to Neumann and Ringsdorf (1986).

The compound *S*-[1,2-bis[(octadecyloxy)carbonyl]ethyl]-cysteamine (precursor of biotin lipid **8**) was prepared in the same manner as the previous ones, but due to its strong tendency for cyclization to the thiomorpholinone, the isolation was avoided, and the chloroform solution of the reaction product was directly used for the preparation of biotin lipid **8**.

The compound *N*,*N*-dioctadecyl-1,3-propanediamine was synthesized by a modified procedure of the method given by Dorn (1981): (1) 3-(dioctadecylamino)propionitrile was prepared by refluxing a solution of 40 mmol of dioctadecylamine in 1.5 mol of acrylonitrile for 2 days under nitrogen. After removal of the excess acrylonitrile by evaporation, the pure product was directly used for the next reaction step. (2) Five grams of $LiAlH_4$ was suspended in 50 mL of diethyl ether, and a solution of 40 mmol of 3-(dioctadecylamino)propionitrile in 100 mL of diethyl ether was added while the reaction mixture was thoroughly chilled in an ice bath and stirred. To complete the reaction, warming to room temperature for 0.5 h was enough. Excess $LiAlH_4$ was eliminated by addition of methanol. The pure *N*,*N*-dioctadecyl-1,3-propanediamine was directly extracted two times with hot $CHCl_3$ (yield 67% for both steps) and used directly for the reaction with BNHS.

Synthesis of Biotinylated Amino Lipids. To a 0.5 mmol solution of the amino precursor compound in 50 mL of $CHCl_3$/2-propanol (2:1), 0.6 mmol of biotinyl-*N*-hydroxysuccinimide and 100 μL of triethylamine were added. By slight warming and ultrasonication, the compounds were dissolved to a clear solution. The mixture was then stirred for 1 h to complete the reaction. The extent of the reaction was monitored by thin-layer chromatography (TLC), with the same solvent mixture as in the flash chromatography. In the case of biotin lipids **7** and **8**, a considerable amount of cyclization product (thiomorpholinone) is formed during the reaction which decreases the yield of these biotin lipids. Upon completion of the reaction, the mixture was washed once with 1 N HCl (acid and noncharged biotin lipids **4**, **6**, **7**, and **8**) or 1 N NaOH (biotin lipid **5**) and twice with water to remove the polar impurities. The reaction of DODA with BNHS to yield biotin lipid **4** proceeds very slowly, due to the formation of a tertiary amide bound, so that an overnight reaction time is required.

Biotin lipid **6** is not soluble in either water or chloroform. It precipitates during the washing procedure with 1 N HCl, and the pure compound can thus be directly collected. The biotin lipids **5** and **7** are completely purified by recrystallization twice from acetone. The two noncharged biotin lipids **4** and **8** are purified by flash chromatography with the solvent mixture $CHCl_3$/MeOH (30/1).

N,N-Dioctadecylbiotinamide (**4**): yield 72%; mp 65.5 °C; ^{1}H 400-MHz NMR ($CDCl_3$) δ 0.89 (t, 6 H, CH_3), 1.25 (m, 60 H, CH_2), 1.40–1.50 [m, 6 H, $COCH_2(CH_2)_3CH$], 1.65–1.75 [m, 4 H, CON $(CH_2)_2(CH_2)_2$], 2.30 (t, 2 H, $NCOCH_2$), 2.72 and 2.91 (d and dd, 1 H and 1 H, SCH_2CH), 3.19 [m, 4 H, $CON(CH_2)_2$], 3.28 (m, 1 H, SCH), 4.30 and 4.50 [m, 2 H, $(CH)_2(NH)_2CO$], 4.91 and 5.40 [m, 2 H, $(NH)_2CO$]; IR (KBr) 2920 and 2851 (C–H), 1708 (C=O urea), 1646 (C=O amide), 1468 (C–H) cm^{-1}. Anal. Calcd for $C_{46}H_{89}O_2N_3S$: C 73.83; H, 11.99; N, 5.61; S, 4.28. Found: C, 71.74; H, 11.33; N, 5.77; S, 4.24.

N,N-Dioctadecyl-N′-biotinyl-1,3-propanediamine (**5**): yield 65%; mp 133 °C; ^{1}H 400-MHz NMR ($CDCl_3$) δ 0.87 (t, 6 H, CH_3), 1.28 (m, 60, CH_2), 1.35–1.45 [m, 4 H, $N(CH_2)_2$-$(CH_2)_2$], 1.60–1.80 [m, 6 H, $COCH_2(CH_2)_3CH$], 1.85 (m, 2 H, NCH_2CH_2), 2.18 (t, 2 H, $NHCOCH_2$), 2.37 [t, 4 H, $N(CH_2)_2$], 2.49 (t, 2 H, NCH_2), 2.73 and 2.89 (d and dd, 2 H, SCH_2CH), 3.13 (m, 1 H, SCH), 3.30 (m, 2 H, CH_2NHCO), 4.30 and 4.50 [m, 2 H, $(CH)_2(NH)_2CO$], 5.25 and 5.98 [s, 2 H, $(NH)_2CO$], 7.50 (t, 1 H, NHCO); IR (KBr) 2916 and 2849 (C–H), 1712 (C=O urea), 1644 and 1555 (C=O amide), 1469 (C–H) cm^{-1}. Anal. Calcd for $C_{49}H_{96}O_2N_4S$: C, 73.07; H, 12.01; N, 6.95; S, 3.98. Found: C, 73.21; H, 11.43; N, 6.82; S, 3.65.

N-Biotinyl-S-[1-carboxy-2-[(N,N-dioctadecylamino)-carbonyl]ethyl]cysteine (**6**): yield 71%; mp 160 °C dec; ^{1}H 400-MHz NMR ($CDCl_3$ + 1% CF_3COOH) δ 0.88 (t, 6 H, CH_3), 1.28 (m, 60 H, CH_2), 1.45–1.61 [m, 6 H, $COCH_2$-$(CH_2)_3CH$], 1.68–1.73 [m, 4 H, $(CH_2)_2(CH_2)_2N$], 2.49 (t, 2 H, $NHCOCH_2$), 2.85 and 2.98 (d and dd, 2 H, SCH_2CH), 2.84–2.90 and 3.05–3.11 (m, 4 H, CH_2CHSCH_2COOH), 3.23–3.35 [m, 5 H, $N(CH_2)_2$ and SCH], 3.95 (m, 1 H,

COOHC*H*S), 4.48 and 4.71 [m, 2 H, (*CH*)$_2$(NH)$_2$CO], 5.04 [m, 1 H, COOH(*CH*)(NH)]; IR (KBr) 2919 and 2853 (C–H), 1705 (C=O urea), 1702 (C=O acid), 1646, 1625, and 1531 (C=O amide, 1465 (C–H) cm^{-1}. Anal. Calcd. for $C_{53}H_{98}O_7N_4S_2$: C, 65.94; H, 10.02; N, 5.80; S, 6.63. Found: C, 64.74; H, 10.31; N, 5.79; S, 6.60.

N-Biotinyl-S-[1,2-bis[(octadecyloxy)carbonyl]ethyl]cysteine (**7**): yield 55%; mp 104 °C; ^{1}H 400-MHz NMR ($CDCl_3$) δ 0.87 (t, 6 H, CH_3), 1.28 (s, 60 H, CH_2), 1.52–1.83 [m, 10 H, (*CH*$_2$CH$_2$OCO)$_2$ and COCH$_2$(*CH*$_2$)$_3$CH], 2.28–2.45 (m, 2 H, NHCO*CH*$_2$), 2.65–2.73 (m, 2 H, OCO*CH*$_2$CH), 2.88–2.96 (m, 2 H, S*CH*$_2$CHCOOH), 3.10 and 3.28 (d and dd, 2 H, s*CH*$_2$CH), 3.18 (m, 1 H, SCH), 3.73 (t, 1 H, OCOCHS), 4.04–4.15 [m, 4 H, (CH$_2$OCO)$_2$], 4.34 and 4.52 [m, 2 H, (*CH*)$_2$(NH)$_2$CO], 4.80 and 4.87 [m, 2 H, (NH)$_2$CO], 5.89 (d, 1 H, NH*CH*COOH), 6.51 (s, 1 H, COOH), 6.94 and 7.2 (dd, 1 H, NHCO); IR (KBr) 2918 and 2850 (C–H), 1722 (C=O acid), 1708 (C=O urea), 1645 and 1531 (C=O amide), 1467 (C–H) cm^{-1}. Anal. Calcd for $C_{53}H_{97}O_8N_3S_2$: C, 65.73; H, 10.10; N, 4.34; s, 6.61. Found: C, 65.74; H, 10.06; N, 3.93; S, 6.74.

N-Biotinyl-S-[1,2-bis[(octadecyloxy)carbonyl]ethyl]cysteamine (**8**): yield 51%; mp 123 °C; ^{1}H 400-MHz NMR ($CDCl_3$) δ 0.89 (t, 6 H, CH_3), 1.28 (m, 60 H, CH_2), 1.43 (m, 2 H, COCH$_2$*CH*$_2$), 1.58–1.72 [m, 8 H, (*CH*$_2$CH$_2$OCO)$_2$ and NHCO(CH$_2$)$_2$(*CH*$_2$)$_2$], 2.23 (t, 2 H, s*CH*$_2$CH$_2$), 2.65–2.99 (m, 6 H, *CH*$_2$NHCO*CH*$_2$ and CH$_2$S), 3.14 (m, 1 H, SCH), 3.48 (m, 2 H, OCO*CH*$_2$CH), 3.68 (t, 1 H, OCOCH$_2$*CH*), 4.05–4.14 [m, 4 H, (CH$_2$OCO)$_2$], 4.31 and 4.50 [m, 2 H, (*CH*)$_2$(NH)$_2$CO], 5.04 and 5.9 [s, 2 H, (NH)$_2$CO], 6.5 (s, 1 H, NHCO); IR (KBr) 2919 and 2850 (C–H), 1734 (C=O ester), 1707 (C=O urea), 1646 and 1550 (C=O amide), 1468 (C–H) cm^{-1}. Anal. Calcd for $C_{52}H_{97}O_6N_3S_2$: C, 67.56; H, 10.58; N, 4.55; S, 6.94. Found: C, 67.53; H, 10.19; N, 4.62; S, 7.31.

Synthesis of the Water-Soluble Biotin Derivatives **9** *and* **10**. A total of 2 mmol of BNHS was dissolved in DMF (dimethylformamide) at room temperature, and 7 mmol of ethanolamine or diethanolamine was added for synthesis of biotin derivatives **9** and **10**, respectively. After completion of the reaction, DMF was removed under vacuum, and the crude product was recrystallized twice from 2-propanol. *N,N*-Bis(2-hydroxyethyl)biotinamide (**10**) required an overnight reaction time in order to complete the reaction. The pure compounds showed only single spots on TLC after each final purification step.

N-(2-Hydroxyethyl)biotinamide (**9**): yield 71%; mp 155–164 °C; ^{1}H 400-MHz NMR (D_2O) δ 1.41 [m, 2 H, CH*CH*$_2$(CH$_2$)$_2$], 1.55–1.75 [m, 4 H, CHCH$_2$(*CH*$_2$)$_2$], 2.27 (t, 2 H, *CH*$_2$CONH), 2.78 and 3.0 (d and dd, 2 H, SCH$_2$), 3.31 (m, 3 H, SCH and CONH*CH*$_2$), 3.62 (t, 2 H, *CH*$_2$OH), 4.4 and 4.6 [m, 2 H, (*CH*NH)$_2$CO]; IR (KBr) 1711 (C=O urea), 1646 and 1559 (C=O amide), 1469 and 1463 (C–H) cm^{-1}. Anal. Calcd for $C_{12}H_{21}O_3N_3S$: C, 50.17; H, 7.37; N, 14.62; S, 11.15. Found: C, 50.14; H, 7.40; N, 14.71; S, 11.66.

N,N-Bis(2-hydroxyethyl)biotinamide (**10**): yield 68%; mp 145–152 °C; ^{1}H 400-MHz NMR (D_2O) δ 1.43 [m, 2 H, CH*CH*$_2$(CH$_2$)$_2$], 1.58–1.76 [m, 4 H, CHCH$_2$(*CH*$_2$)$_2$], 2.49 (t, 2 H, *CH*$_2$CONH), 2.78 and 2.97 (d and dd, 2 H, SCH$_2$), 3.33 (m, 1 H, SCH), 3.51 and 3.59 [t, 4 H, CON(CH$_2$)$_2$], 3.69 and 3.73 [t, 4 H, (*CH*$_2$OH)$_2$], 4.4 an 4.59 [m, 2 H, (*CH*NH)$_2$CO]; IR (KBr) 1706 (C=O urea), 1649 (C=O amide), 1467 (C–H) cm^{-1}. Anal. Calcd for $C_{14}H_{25}O_4N_3S$: C, 50.74; H, 7.60; N, 12.67; S, 9.67. Found: C, 50.58; H, 7.06; N, 12.73; S, 10.40.

General Characterization Methods. Melting points of synthesized compounds were determined with Büchi apparatus and are uncorrected. Nuclear magnetic resonance spectra (NMR) were recorded on a Bruker AM 400 (400 MHz) spectrometer. The chemical shifts are given in parts per million (ppm) (δ) relative to tetramethylsilane. Infrared spectra were taken with a Nicolet 5DXC FT-IR spectrometer. For the UV spectrometric titration of avidin with biotin derivatives, a Perkin-Elmer Lambda 5 UV/vis spectrophotometer was used. The microanalysis were performed by Microanalysis Laboratories, Universität Mainz.

Protein Modification. Streptavidin and avidin were labeled with FITC as described by Nargessi and Smith (1986) by using a molar ratio of 1:1 streptavidin or avidin to FITC. Succinylation of avidin was performed according to the method described by Hofmann et al. (1980).

Monolayer Experiments. For characterization of the monolayers, a computer-controlled film balance was used (Albrecht, 1983). The pure biotin lipids were spread from $CHCl_3$ solutions having concentrations of approximately 0.4 mg/mL. The water used as a subphase was distilled three times on glass and then purified by a Milli-Q water purification system (Millipore). Its resistivity was higher than 18 M Ω cm.

The hysteresis experiments were performed on the same trough, at 30.0 ± 0.2 °C with a subphase containing 0.5 M NaCl. After the biotin lipids were spread, the film was expanded in the gas-analogue state, and 1 mg of streptavidin or avidin in 5 mL of NaCl solution was injected into the subphase. An incubation time of about 2 h was found to be enough to enable the protein to distribute homogeneously in the subphase and to bind or adsorb to the lipid monolayer. The hysteresis experiment was then performed as follows: (1) compression to 40 mN/m; (2) immediate decompression to the largest molecular area; (3) incubation for 40 min; (4) recompression until collapse. The compression speed used was 4.5 Å^2/(molecule min).

Fluorescence Microscopy of the Monolayers. For direct observation of lipid monolayers, a special Langmuir trough in combination with a fluorescence microscope was used (Meller, 1988). In analogy to the hysteresis experiment, after spreading, the lipid layer was expanded to the gas-analogue state, and 0.1 mg of fluorescein-labeled streptavidin in 5 mL of solution was injected into the subphase at 30 °C.

UV Spectrometric Titration of Avidin. This binding assay (Green, 1963) was used to test the binding capability of biotin to avidin, streptavidin, and succinylated avidin as well as to study the binding of the biotin lipids **4**, **5** (pH 3 and 11), **7** and, **8** and the biotin derivatives **9** and **10** to avidin. In order to prepare aqueous solutions of the biotin lipids, two detergents, octyl glucoside and emulphogene BC-720, were used. The biotin lipids (0.15 mM) were dissolved in a solution containing 50 mM NaCl and 30 mM octyl glucoside (cmc = 25 mM) or 4 mM emulphogene BC-720 (cmc = 0.087 mM). Equal volumes of avidin (0.2 mg/mL), in the same buffer and detergent system, were placed in two 1-cm quartz cuvettes. Then, difference spectra between 210 and 250 nm were recorded after addition and appropriate mixing of each 20-μL aliquot of the biotin lipid solution (20 μL of buffer was also added to the reference cuvette). Maximum binding capacity is reached when a plateau is observed. With this quantitative titration, avidin and streptavidin were found to give a biotin: protein ratio of 3.5 and 3.8, respectively.

Results and Discussion

Biotin lipids **1** and **3**—which differ only in the chain length

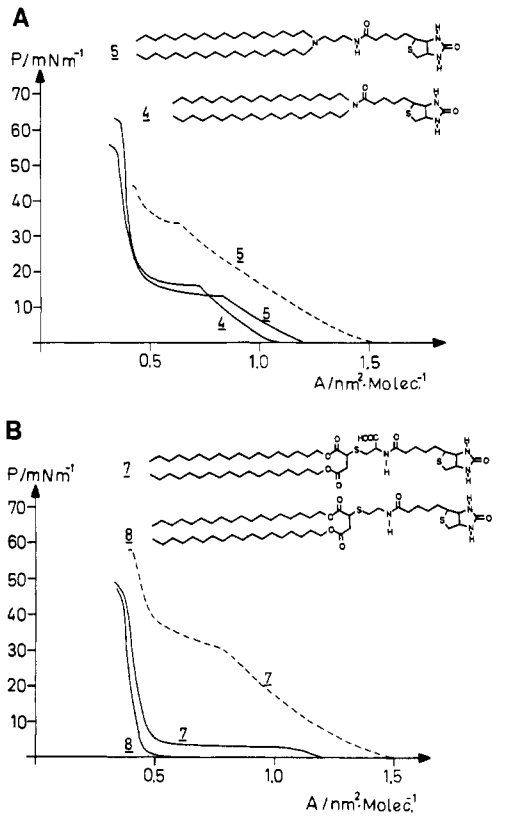

FIGURE 1: Surface pressure/area isotherms of biotin lipids **4** and **5** (A) and of biotin lipids **7** and **8** (B) on pure water at pH 5.5 (—), at pH 3 [(--) biotin lipid **5** (A)] and at pH 11 [(--) biotin lipid **7** (B)]. Temperature: 30.0 ± 0.2 °C.

of their hydrophobic core (Chart I)—exhibit very similar monolayer behavior at 30 °C. The only difference is that biotin lipid **3** shows a phase transition at a lower surface pressure than biotin lipid **1**, because longer fatty acid chains lower the surface pressure of the phase transition (results not shown).

In order to compare biotin lipids **4** and **5** (Figure 1A), one must be certain that the tertiary amine of biotin lipid **5** (Chart I) does not bear a charge at pH 5.5. The isotherm of biotin lipid **5** at pH 5.5, shown in Figure 1A, is identical with the one measured at pH 11. However, a very drastic change is observed at pH 3 (Figure 1A, broken line). At this pH, the molecular area of biotin lipids **5** is ~30 Å^2/molecule larger than at pH 5.5 or 11. Moreover, at pH 5.5 or 11, the phase transition of biotin lipid **5** (Figure 1A) takes place at a surface pressure of 12 mN/m as compared to 33.3 mN/m at pH 3. These two observations strongly suggest that the tertiary amine of biotin lipid **5** bears only a charge at pH 3. Therefore, at pH 5.5, biotin lipid **5** is not significantly charged and can be compared with biotin lipid **4**.

As can be seen in Chart I, the only difference between biotin lipids **4** and **5** is that biotin lipid **5** contains an aminopropyl spacer which decouples the biotin molecule from the dioctadecylamine hydrophobic core. The presence of such a spacer in the polar headgroup usually leads to a higher surface pressure of the phase transition (Laschewski et al., 1987). However, the phase transition of biotin lipids **5** (12 mN/m) takes place at a lower surface pressure than in the case of biotin lipid **4** (15.5 mN/m, Figure 1A). This experimental observation can be explained by the formation of hydrogen bonds between the secondary amides of the aminopropyl spacers. The smaller molecular area of biotin lipid **5** in the solid condensed state, as compared to that of biotin lipid **4**, supports this interpretation. Indeed, such a hydrogen belt should lead to better packing of the monolayer which should, in turn, prevent the achievement of a higher phase transition surface pressure. Moreover, the measurement of a much higher melting point for biotin lipid **5** (133 °C) than for biotin lipid **4** (65.5 °C) argues also in favor of this explanation.

Figure 1B presents the comparison between isotherms of biotin lipids **7** and **8** whose chemical structures only differ in one carboxylic acid group in the polar head moiety (Chart I). This carboxylic acid group of biotin lipid **7** is not significantly dissociated at pH 5.5. Indeed, the isotherms of biotin lipid **7** at pH 3 and 5.5 are identical whereas a drastic change is observed at pH 11 (broken line). At this pH, the molecular area at the beginning of the isotherm is ~30 Å^2/molecule larger than at pH 3 or 5.5. Moreover, at pH 3 and 5.5, the phase transition of biotin lipid **7** takes place at a surface pressure of 2.9 mN/m as compared to 30.8 mN/m at pH 11. These two observations strongly suggest that biotin lipid **7** does not bear a charge at pH 5.5. Therefore, at this pH, biotin lipid **7** can be compared with biotin lipid **8**.

The larger molecular area of biotin lipid **7**, as compared to biotin lipid **8** (Figure 1b), suggests that its additional carboxylic acid group (Chart I) induces a looser packing of the monolayer. Moreover, the effect of this carboxylic acid group on the phase transition temperature of biotin lipid **7** can be estimated from the surface pressure isotherms. Indeed, the relative difference between the phase transition temperature of biotin lipid **7** and **8** can be evaluated as follows: at 30 °C, as stated above, the phase transition of biotin lipid **7** occurs at 2.9 mN/m (Figure 1B); biotin lipid **8** shows a phase transition at a similar surface pressure only at 35 °C (data not shown). The phase transition temperature of biotin lipid **7** should therefore be about 5 °C lower than the one of biotin lipid **8**. This reduction of the phase transition temperature by the addition of a carboxylic acid group is also consistent with the observation of a looser packing of the monolayer.

Biotin Lipid–Streptavidin Interaction at the Air–Water Interface. The purpose of this study is to simulate a surface recognition process by the monolayer technique as a model membrane system. In order to achieve this goal, it is important to distinguish the specific interaction of the subphase-solubilized streptavidin with the biotin lipid monolayer (recognition process) from its nonspecific adsorption at the air–water interface. The basic concept to discriminate between the two interactions is to use the active form of streptavidin, in comparison with the inactivated form, where the latter is saturated with four bound biotin molecules. Indeed, the active streptavidin can undergo a specific interaction with the biotin lipid monolayer whereas the inactivated one [streptavidin–(biotin)$_4$ complex] can only adsorb nonspecifically on the monolayer and thus serve as a negative control. The very high affinity binding of the streptavidin–biotin complex allows the assumption that the above concept is valid.

A large difference, therefore, should be observed in the monolayer behavior of the biotin lipids when either the active streptavidin or the inactivated one is used. However, in order to assess the validity of this concept, a control experiment involving a non biotin lipid was performed. In this case, no difference between the monolayer behavior of the non biotin lipid (dipalmitoylphosphatidylcholine, DPPC) in the presence of either active or inactivated forms of streptavidin or avidin has been observed because no specific interaction can occur (results not shown). Nevertheless, a weak nonspecific protein adsorption was observed, leading to a small increase of the molecular area of pure DPPC.

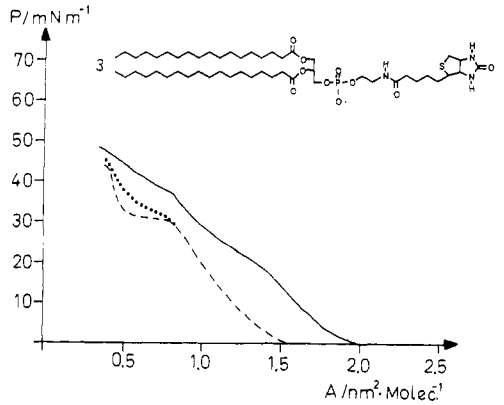

FIGURE 2: Surface pressure/area isotherms of biotin lipid **3** on 0.5 M NaCl solution (pH 5.5) at 30.0 ± 0.2 °C: pure lipid (– –); subphase containing 1 mg of active streptavidin (—); subphase containing 1 mg of inactivated streptavidin (···).

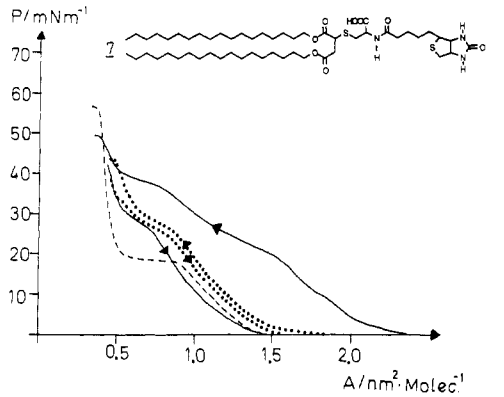

FIGURE 3: Surface pressure/area isotherms of biotin lipid **7** on 0.5 M NaCl solution (pH 5.5) at 30.0 ± 0.2 °C: pure lipid (– –); subphase containing 1 mg of active streptavidin—decompression and recompression (—); subphase containing 1 mg of inactivated streptavidin—decompression and recompression (···).

Recognition of Three Different Biotin Lipids by Streptavidin at the Air–Water Interface. (A) Biotin Lipid **3***–Streptavidin Interaction.* Figure 2 shows the surface pressure isotherm of biotin lipid **3** before (broken line) and after the injection of active (solid line) or inactivated streptavidin (dotted line) in the subphase. It can be seen that the presence of active streptavidin leads to a very large increase in the molecular area of biotin lipid **3** (solid line). Either specific or nonspecific interactions can be responsible for this effect. However, the possibility that nonspecific interactions take place can be ruled out with the inactivated streptavidin experiment. Indeed, the isotherm of the pure lipid (broken line) remains nearly unchanged in the presence of inactivated streptavidin (dotted line). This strongly suggests that the inactivated streptavidin shows neither specific nor nonspecific interaction with the biotin lipid **3** monolayer. Therefore, drastic changes observed in the presence of active streptavidin (solid line) are very likely to be caused by the specific binding of streptavidin to the biotin lipid **3** monolayer.

(B) Biotin Lipid **7***–Streptavidin Interaction.* Hysteresis experiments are introduced in Figure 3 in order to show that they are useful to discriminate the specific and nonspecific biotin lipid–streptavidin interactions. After injection and incubation of the protein in the subphase, the film is compressed to 40 mN/m, decompressed to the maximum molecular area, and recompressed until collapse (the first compression, being very similar to the recompression, is always left out to avoid overlapping and to increase clarity).

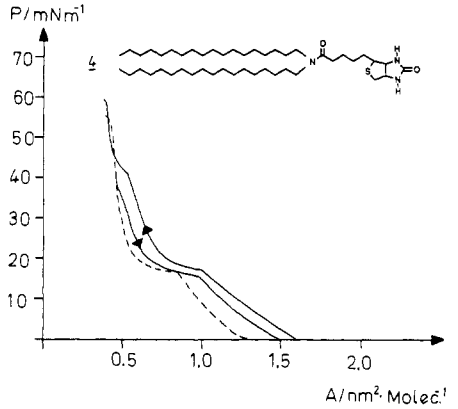

FIGURE 4: Surface pressure/area isotherms of biotin lipid **4** on 0.5 M NaCl solution (pH 5.5) at 30.0 ± 0.2 °C: pure lipid (– –); subphase containing 1 mg of active or inactivated streptavidin—decompression and recompression (—).

The two curves (solid and dotted line) are the hysteresis isotherms of biotin lipid **7** in the presence of active and inactivated streptavidin, respectively. In the presence of active streptavidin (solid line), a large hysteresis effect is observed; i.e., a large difference exists between the molecular area of the recompression curve and that of the decompression curve. However, inactivated streptavidin causes only a very small hysteresis effect. In fact, in this case, both curves (recompression and decompression) are very similar. This difference can be explained as follows: when streptavidin is specifically bound to biotin lipid **7** (solid line), the monolayer relaxes much slower upon decompression than when only nonspecific adsorption is possible (dotted line). It is, therefore, very likely that the binding is responsible for this large hysteresis effect.

Moreover, it is noteworthy that the molecular area of biotin lipid **7** is increased much more in the presence of active streptavidin (solid line) than in the presence of inactivated streptavidin (dotted line). It is thus clear that the strong specific binding effect of streptavidin on the monolayer is overlapped by a weak nonspecifc adsorption of streptavidin. Therefore, the hysteresis experiment and the use of the inactivated form of streptavidin enable discrimination of both phenomena. Furthermore, this observation of specific biotin lipid **7**–streptavidin binding is supported by UV titration and fluorescence microscopy experiments.

By fluorescence microscopy, as will be discussed below, it was possible to observe oriented two-dimensional domains of biotin lipid **7**–streptavidin in the air–water interface. This result strongly suggests that specific binding takes place. Conversely, no fluorescence has been observed when inactivated streptavidin was used.

Furthermore, the binding of biotin to streptavidin (or avidin) is accompanied by a red shift of the 230-nm protein absorption band. Thus, measurement of a difference spectrum allows titration of the four binding sites of streptavidin (or avidin) with biotin (Green, 1963). Similarly, the streptavidin (or avidin) binding sites can also be titrated with the biotin lipids. Biotin lipid **7** was thus dissolved in a micellar solution of emulphogene or octyl glucoside. The measurement is then performed at pH 3 and 11. As shown above, biotin lipid **7** does not bear a charge at pH 3 whereas it is negatively charged at pH 11. Nevertheless, both the charged and uncharged forms of biotin lipid **7** can quantitatively titrate streptavidin (or avidin) whatever the detergent used. These results are therefore consistent with the monolayer experiments. Biotin lipid **8**, the analogous lipid to biotin lipid **7** (see Chart I), showed also quantitative titration at pH 5.5. Since streptavidin

and avidin were found to give identical results, only avidin was used in the subsequent titration experiments.

(C) *Biotin Lipid* **4**–*Streptavidin Interaction.* The isotherm of pure biotin lipid **4** (broken line) as well as its hysteresis isotherms in the presence of active and inactivated (solid line) streptavidin are presented in Figure 4. It can be seen that the presence of streptavidin or inactivated streptavidin increases slightly the molecular area of biotin lipid **4**. Moreover, the hysteresis isotherms of biotin lipid **4** in the presence of active and inactivated streptavidin are almost identical. Therefore, only one is shown here (solid line). This similarity strongly suggests that both active and inactivated streptavidin undergo only nonspecific adsorption on the biotin lipid **4** monolayer. Thus, no specific binding can take place between active streptavidin and biotin lipid **4**. This conclusion is supported by the UV titration. Indeed, no reaction between biotin lipid **4** and avidin (or streptavidin) could be measured by UV titration in the two different detergents used. These results very strongly suggest that biotin lipid **4** does not specifically interact with streptavidin.

Two hypotheses were put forward to explain this behavior. The accessibility of the biotin headgroup for binding by streptavidin can be prevented by (1) a steric hindrance caused by the tertiary amide bond of biotin lipid **4** or (2) the lack of a spacer between the biotin molecule and the hydrophobic dioctadecylamine in biotin lipid **4**.

The first hypothesis was tested by measuring the binding capability of the water-soluble biotin derivatives **9** and **10** by UV titration. If steric hindrance inhibits the binding, biotin derivative **9** should bind streptavidin whereas derivative **10** should not. However, both biotin derivatives **9** and **10**, containing respectively a secondary and tertiary amide group, exhibited full binding capability toward avidin as shown by UV spectrometric titration. Therefore, it can be concluded that the tertiary amide bond of biotin lipid **4** is not responsible for its nonbinding ability toward avidin.

The second hypothesis was tested by synthesizing biotin lipids **5** and **6** which comprise, respectively, a short and a long spacer between the biotin molecule and the hydrophobic dioctadecylamine unit (Chart I). Then, the biotin lipid **5**–streptavidin binding was estimated by hysteresis experiments and UV titration. The measured hysteresis isotherms (results not shown) are similar to those of biotin lipid **7** (Figure 3) where specific binding could be discriminated from nonspecific adsorption. Moreover, in contrast to biotin lipid **4**, it was found that the avidin binding sites could be titrated by biotin lipid **5**. Thus, in conclusion, with biotin lipid **4** streptavidin binding is probably prevented by the lack of a spacer between the hydrophobic tails and the biotin headgroup.

Recognition of Biotin Lipid **7** *by Avidin and Succinylated Avidin at the Air–Water Interface.* It is already known that avidin shows a much stronger nonspecific adsorption than streptavidin, presumably because of its sugar content and also because it bears a negative charge at pH 5.5 (Hofmann et al., 1980; Roffman et al., 1986). Then, one can speculate whether this adsorption behavior of avidin prevents its specific binding to the biotin moiety of the biotin lipid. Hysteresis experiments, performed as described in Figure 3, have shown that specific binding could hardly be discriminated from nonspecific adsorption (results not shown).

This behavior is very different from that of streptavidin. Indeed, inactivated streptavidin showed only a small nonspecific adsorption (Figure 3, dotted line) whereas specific binding of active streptavidin to biotin lipid **7** can clearly be discriminated (Figure 3, solid line). Unlike avidin, which is a basic glycoprotein ($pI \sim 11$), streptavidin is not charged at neutral pH ($pI \sim 7$) and contains no sugar residues. This nonspecific adsorption of avidin can therefore be attributed either to its sugar content (Hiller et al., 1987) or to charge–charge interactions (Wilchek & Bayer, 1988). The contribution of the charge–charge interactions to the nonspecific adsorption of avidin was found to be largely decreased by the use of a subphase containing 0.5 M NaCl as compared to pure water (results not shown). In spite of this, its nonspecific adsorption is still very important. Therefore, avidin was modified by succinylation in order to further decrease these charge–charge interactions.

The reaction of succinic anhydride with the accessible free amino groups of avidin results in amine replacement by free carboxylic acid groups. This procedure leads to a shift of the isoelectric point of avidin to lower pH values. The nonspecific adsorption of avidin, through charge–charge interactions, is significantly decreased by this succinylation process and allows discrimination of the biotin lipid **7**–avidin-specific binding (results not shown). However, the nonspecific adsorption of succinylated avidin is still larger than that in the case of streptavidin. This difference could originate from some remaining charge–charge interactions or from the sugar content of avidin (Hiller et al., 1987).

Observation of Oriented Two-Dimensional Biotin Lipid–Streptavidin Domains by Fluorescence Microscopy. Fluorescence microscopy of lipid monolayers enables direct visualization of monolayer domains formed in the phase transition from the liquid-expanded to the solid-condensed state (Lösche & Möhwald, 1984; McConnell et al., 1984). Analogously, this method can be applied to investigate the surface recognition processes by labeling the ligand molecules with fluorescein. Their nonspecific adsorption or their specific binding with their receptors, located at the gas–water interface, can then be directly followed by fluorescence microscopy.

Figure 5 shows the fluorescence micrographs of the biotin lipid **6**–streptavidin monolayer where only the fluorescence generated by the fluorescein-labeled streptavidin is observed. It can be seen that the streptavidin molecules self-organize to form regular, H-like-shaped domains. In all cases they exhibit two main axes of different lengths. These domains only form if a biotin lipid receptor is present at the air–water interface. That is, no domains could be observed when the same experiment is performed with a DPPC monolayer.

The fluorescence intensity of these different domains is strongly dependent on the angle of polarization of the exciting light. Both panels show the same domains except that there is a 90° difference in the state of polarization of the light between panels A and B of Figure 5. This results in the observation of optical anisotropy of the domains. This phenomenon is easier to visualize when perpendicularly oriented domains are compared. Indeed, one dark domain and its perpendicularly oriented, bright neighbor (see arrows, Figure 5A) become respectively bright and dark (Figure 5B) when the polarizer is rotated by 90°, demonstrating complete inversion of fluorescence intensity. The fluorescence intensity of the other domains is dependent upon their macroscopic orientation as well. This implies that the orientation of streptavidin is the same in all domains and that oriented, two-dimensional biotin lipid–streptavidin domains, as schematically illustrated in Figure 5C, are formed. Both observations, their optical anisotropy and their regular shape, strongly suggest that the streptavidin domains are highly ordered and, might we speculate, are two-dimensional crystals (see Added in Proof).

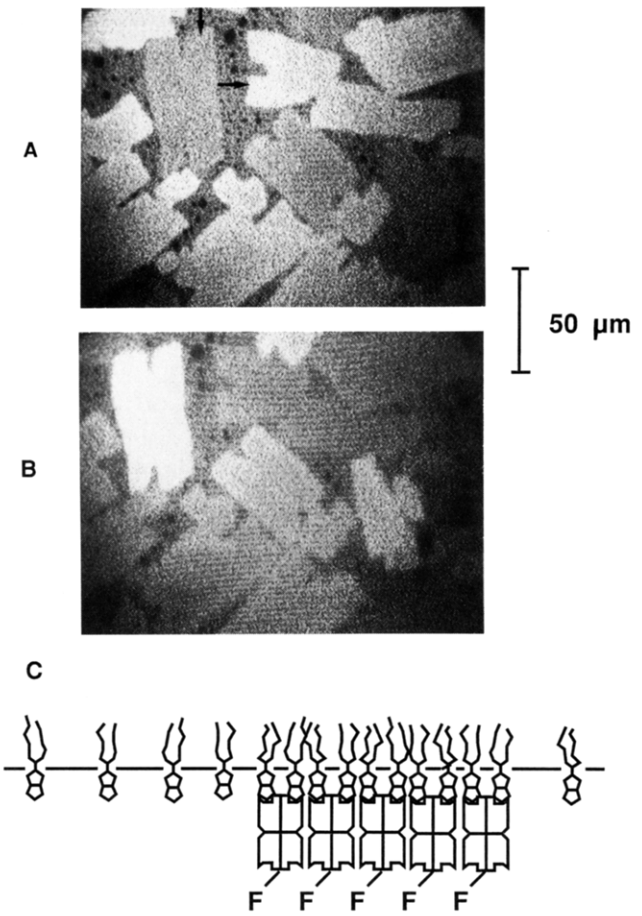

FIGURE 5: Fluorescence micrographs of oriented two-dimensional biotin lipid **6**–fluorescein-labeled streptavidin domains at the air–water interface (pH 5.5, 0.5 M NaCl, 30.0 ● 0.2 °C). The state of polarization of light in micrograph A is phased shifted by 90° compared to that in micrograph B. The arrows in (A) show perpendicularly oriented domains. (C) shows a schematic representation of the domains' structure.

Figure 5C also shows that, as is required from the light polarization effects on the domains' fluorescence, the fluorescein molecules, which are covalently attached to streptavidin, have the same orientation. However, this is rather surprising because the streptavidin molecules are randomly labeled. Thus, this can be explained by either the fact that the fluorescein molecules can only bind to the same free amino group in the protein or the fact that the formation of these domains forces a critical percentage of the labels into a certain order detected in the surface domains.

Furthermore, the presence of a highly oriented monolayer, e.g., the solid-condensed state, is not necessary for observation of the formation of anisotropic domains. The domains shown in Figure 5A,B are, indeed, formed in the gas state of the biotin lipid **6** monolayer. Upon compression, the macroscopic structure of these domains is destroyed at a surface pressure of ~20 mN/m seen in both protein–lipid recompression curves in Figures 2 and 3. This result strongly suggests that the destruction of these protein domains has a larger effect on the compressibility of the monolayer.

A schematic representation of the proposed mechanism for the formation of these oriented two-dimensional biotin lipid–streptavidin domains is presented in Figure 6. As a first step, the streptavidin molecules bind specifically to the biotin lipid headgroups (Figure 6A). Then, by diffusing in the plane of the monolayer, another binding site of the streptavidin molecule in this biotin lipid$_1$–streptavidin complex is allowed to react with a second biotin lipid (Figure 6A). Subsequently,

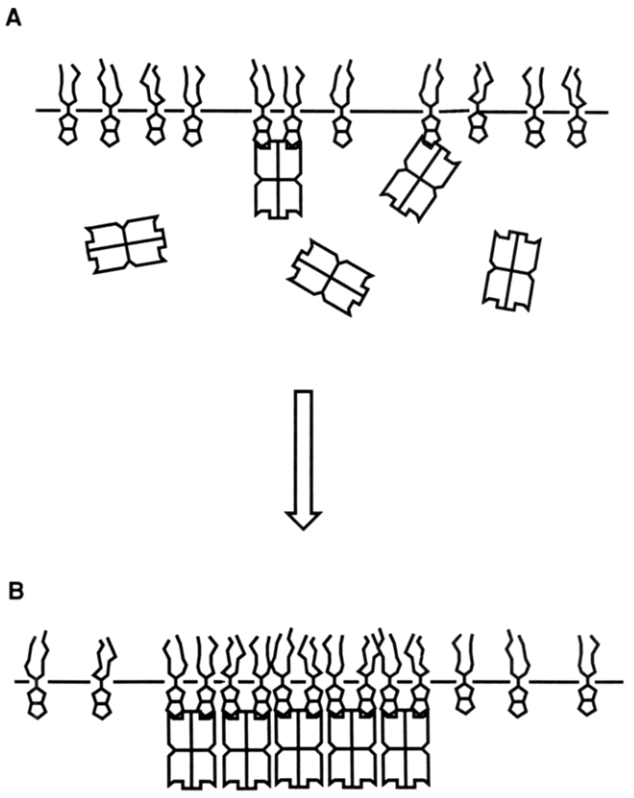

FIGURE 6: Proposed mechanism for the formation of the two-dimensional biotin lipid–streptavidin domains: (A) specific binding and preorientation of streptavidin molecules; (B) formation of two-dimensional protein domains.

the biotin lipid$_2$–streptavidin complexes keep diffusing until they meet and form two-dimensional protein domains (Figure 6B).

Fluorescence microscopy measurements of biotin lipid **7**–streptavidin have also been performed. In this case, optical anisotropy of the domains has also been observed. However, with fluorescein-labeled avidin, instead of streptavidin, neither domains nor optical anisotropy of the homogeneous surface fluorescence has been observed. As suggested from the hysteresis experiments, the strong nonspecific adsorption of avidin on biotin lipid **7** monolayers could be responsible for this very different behavior as compared to that of streptavidin. Then, the specific binding, if any takes place, is obviously hidden by the nonspecific adsorption. We are, therefore, currently trying to deglycosylate avidin, as performed by Hiller et al. (1987), in order to decrease nonspecific adsorption and induce formation of two-dimensional avidin domains.

Added in Proof

By electron microscopy, it was shown, in collaboration with the group of R. D. Kornberg (M. Ahlers, R. Blankenburg, S. A. Darst, R. D. Kronberg, E. W. Kubalek, H. O. Ribi, and H. Ringsdorf, submitted for publication), that these domains are two-dimensional crystals of streptavidin bound to the biotin lipid layer. The streptavidin three-dimensional structure determined by electron crystallography from the crystals reveals the location of the four biotin binding sites on each streptavidin tetramer with respect to the lipid membrane. Two of the sites, which face the membrane surface, are utilized in the streptavidin–lipid complex while the other two sites, which face away from the membrane, are free and exposed to the aqueous solution. The free sites can be specifically labeled with biotinylated ferritin, indicating that the streptavidin–biotinylated lipid system may serve to concentrate and orient

specifically biotinylated macromolecules on a lipid layer, facilitating their crystallization in two dimensions.

REFERENCES

Albrecht, O. (1983) *Thin Solid Films 99*, 227-232.
Bayer, E. A., & Wilchek, M. (1974) *Methods Enzymol. 34*, 265-267.
Bayer, E. A., Rivnay, B., & Skutelsky, E. (1979) *Biochim. Biophys. Acta 550*, 464-473.
Cuatrecasas, P., & Wilchek, M. (1968) *Biochem. Biophys. Res. Commun. 33*, 235-239.
Dorn, K. (1981) PhD-Dissertation, Mainz Universität.
Garlick, R. K., & Giese, R. W. (1988) *J. Biol. Chem. 263*, 210-215.
Green, N. M. (1963) *Biochem. J. 89*, 599-604.
Green, N. M. (1975) *Adv. Protein Chem. 29*, 85-133.
Hashimoto, K., Loader, J. E., & Kinsky, S. C. (1986) *Biochim. Biophys. Acta 856*, 556-565.
Hiller, Y., Gershoni, J. M., Bayer, E. A., & Wilchek, M. (1987) *Biochem. J. 248*, 167-171.
Hofmann, K., Wood, S. W., Brinton, C. C., Montilbeller, J. A., & Finn, F. M. (1980) *Proc. Natl. Acad. Sci. U.S.A. 77*, 4666-4668.
Laschewski, A., Ringsdorf, H., Schmidt, G., & Schneider, J. (1987) *J. Am. Chem. Soc. 109*, 788-796.
Lösche, M., & Möhwald, H. (1984) *Rev. Sci. Instrum. 55*, 1968-1972.
Loughrey, H., Bally, M. B., & Cullis, P. R. (1987) *Biochim. Biophys. Acta 901*, 157-160.
McConnell, H. M., Tamm, L. K., & Weis, R. W. (1984) *Proc. Natl. Acad. Sci. U.S.A. 81*, 3249-3253.
Meller, P. (1988) *Rev. Sci. Instrum. 59*, 2225-2231.
Nargessi, R. D., & Smith, D. S. (1986) *Methods Enzymol. 122*, 67-72.
Neumann, R., & Ringsdorf, H. (1986) *J. Am. Chem. Soc. 108*, 487-490.
Reed, R. A., Mattai, J., & Shipley, G. G. (1987) *Biochemistry 26*, 824-832.
Ribi, H. O., Reichard, P., & Kornberg, R. D. (1987) *Biochemistry 26*, 7974-7979.
Ribi, H. O., Ludwig, D. S., Lynne Mercer, K., Schoolnik, G. K., & Kornberg, R. D. (1988) *Science 239*, 1272-1276.
Roffman, E., Meromsky, L., Ben-Hur, H., Bayer, E. A., & Wilchek, M. (1986) *Biochem. Biophys. Res. Commun. 136*, 80-85.
Uzgiris, E. E. (1987) *Biochem. J. 242*, 293-296.
Uzgiris, E. E., & Kornberg, R. D. (1983) *Nature 301*, 125-129.
Wilchek, M., & Bayer, E. A. (1988) *Anal. Biochem. 171*, 1-32.

Kinetics of the Purified Glucose Transporter. Direct Measurement of the Rates of Interconversion of Transporter Conformers†

James R. Appleman*,‡ and Gustav E. Lienhard§

Department of Biochemical and Clinical Pharmacology, St. Jude Children's Research Hospital, Memphis, Tennessee 38101, and Department of Biochemistry, Dartmouth Medical School, Hanover, New Hampshire 03756

Received April 5, 1989; Revised Manuscript Received June 1, 1989

ABSTRACT: There is considerable evidence that the mechanism of glucose transport by the transporter of human erythrocytes is one in which the transporter oscillates between two conformations, T_o and T_i. Each conformer possesses a single glucose binding site that in vivo faces either the extracellular space (conformer T_o) or the cytoplasm (conformer T_i). In this study, the interconversions of these conformers in the absence and presence of D-glucose have been directly observed by means of the stopped-flow method with fluorescence detection. Nearly unidirectional conversion of one conformer to the other was accomplished by rapidly mixing purified transporter (a mixture of T_o and T_i) with either 4,6-ethylidene-D-glucose, which preferentially binds to T_o, or phenyl β-D-glucoside, which preferentially binds to T_i. The values of the individual rate constants for the conversion of T_i to T_o and vice versa in the absence and presence of D-glucose at 10.0 °C have been obtained, and these show that the kinetics are consistent with the alternating conformation model for transport. Conformational change occurs much more rapidly with glucose bound to the transporter. Furthermore, the activation energy E_a for conformer interconversion is much less when glucose is bound than for unliganded transporter. For example, E_a is approximately 28 kcal/mol for $T_i \rightarrow T_o$ versus 17 kcal/mol for $T_i + S \rightarrow T_oS$, where S is glucose. The α-anomer of glucose was 37% more effective than the β-anomer in speeding the interconversion. Analysis of the fluorescence change upon mixing the transporter with several concentrations of 4,6-ethylidene-D-glucose revealed that the intrinsic fluorescence of the T_o form is less than that of the T_i form by 20% or more.

The glucose transporter of human erythrocytes is a transport system of the facilitated diffusion type that can be purified in abundance (Baldwin et al., 1982). The amino acid sequence of the transporter indicates that the polypeptide chain weaves across the membrane 12 times (Mueckler et al., 1985). The mechanism of transport is most probably one in which the transporter oscillates between two conformations. One conformer, T_o, exhibits an extracellular glucose binding site. The other conformer, T_i, exhibits an inward-facing glucose binding

† This work was supported by Research Grant GM 22996 (to G.E.L.) from the National Institutes of Health.

‡ St. Jude Children's Research Hospital.
§ Dartmouth Medical School.

0006-2960/89/0428-8221$01.50/0